RGG-motif proteins regulate mRNA translation upon genotoxic stress

Raju Roy^[1], Gayatri Mohanan^[1], Hélène Malka-Mahieu[2,3], Anusmita Biswas[1], Celine Labbe[2], Stéphan Vagner*,[2,3] and Purusharth I Rajyaguru*,[1]

[1]Department of Biochemistry, Indian Institute of Science, Bangalore 560012

[2]Institut Curie, PSL Research University, CNRS UMR3348, INSERM U1278, F-91405, Orsay, France

[3]Université Paris Sud, Université Paris-Saclay, CNRS UMR3348, INSERM U1278, F-91405 Orsay, France

^Authors have contributed equally

*Correspondence: rajyaguru@iisc.ac.in; Stephan.vagner@curie.fr

Keywords: Hydroxyurea, genotoxic stress, RGG-motif proteins, translation control, stress response, yeast, post-transcriptional gene regulation, RNA granules

Abstract

RGG motif-containing proteins are the second largest group of RNA-binding proteins. These proteins have been implicated in several cellular processes. Here we identify a new role of yeast RGG-motif proteins Sbp1, Scd6, and its human ortholog LSM14A, in genotoxic stress response. Scd6 and Sbp1 colocalize to cytoplasmic puncta upon hydroxyurea (HU) treatment, and Scd6 is required for the efficient localization of Sbp1. These puncta are reversible and require RNA for their assembly. The RGG-motif is important for the localization of both proteins to puncta. Strikingly, the absence of Scd6 increases HU tolerance under normal conditions but sensitizes the cells to HU upon overexpression of Srs2, which is known to dampen the response to DNA damage. LSM14A also localizes to puncta in response to genotoxic stress such as HU and cisplatin. This localization also depends on the two RGG motifs of LSM14A. While proximity ligation assay reveals that LSM14A is associated with the translation initiation factor eIF4G, polysome profiling experiments followed by RNA sequencing identify numerous transcripts that are regulated by LSM14A at the translational level under normal conditions and in response to HU. Our work identifies RGG motif-containing proteins as key players in orchestrating genotoxic stress response by determining the translation status of a subset of mRNAs.

Introduction

DNA damage caused by cellular conditions and/or exogenous factors leads to genomic instability and, thereby, genotoxic stress. Replication errors, defective DNA damage repair, and nucleotide misincorporation are some of the cellular events leading to DNA damage [1] Exogenous factors causing DNA damage include exposure to genotoxins such as hydroxyurea, cisplatin, etc. Living systems employ strategies to regulate different gene expression steps to alter the cellular proteome allowing it to mount an effective genotoxic stress response (GSR). The contribution of various gene expression steps to GSR is well documented, however changes in the fate of cytoplasmic mRNAs in response to GSR remain poorly explored [2].

RNA binding proteins (RBPs) play a key role in determining the functional states of mRNA. Several classes of RNA binding domains such as RNA Recognition Motif (RRM), KH-domain, Zn-finger motif and PUMILIO have been reported to play a role in post-transcriptional gene control by affecting specific subsets of mRNAs. RGG motif-containing proteins are the second largest class of RBPs that are also implicated in binding to proteins and DNA [3,4] RGG-motifs, are characterized by repeats of RGG-/RGX- that impart properties

of low-complexity sequences[3]. Consistently, these sequences contribute towards the assembly of ribonucleoprotein (RNP) condensates (*i.e.*, RNA granules) by undergoing liquid-liquid phase separation [5] In yeast, processing bodies (P-bodies or PB) and stress granules (SG) are the major cytoplasmic mRNPs formed in response to several physiological cues. They contain several RNA and RBPs. PBs are reported to be sites of mRNA decay, whereas SGs are implicated in mRNA storage and repression. *S. cerevisiae* Sbp1 and Scd6 are two RBPs with RGG-motif sequences that target eIF4G to repress translation. Scd6 is a known P-body and stress granule resident protein in response to glucose deprivation and oxidative stress. The RGG-motif of these proteins is important for localization to RNA granules such as P bodies, interaction with eIF4G and consequently for translation repression activity [6,7] Interestingly, RGG-motif of Sbp1 has recently been implicated in P-body disassembly suggesting that RGG-motifs can promote both assembly and disassembly of RNA granules [8] LSM14A, the human ortholog of Scd6 is a granule-resident protein which has also been implicated in translational control [9] Interestingly LSM14A contains two RGG-motifs as compared to a single RGG-motif in Scd6 [10] LSM14A plays a key role in formation of the mRNA silencing complex via its association with DDX6 [11] Although xRAP55 (Xenopus ortholog of LSM14/Scd6) has been reported to repress translation [12], the direct role of human LSM14 in translational repression remains to be demonstrated. Interestingly LSM14A has been reported as a sensor of viral nucleic acid which plays a key role in antiviral response [13] Scd6 is known to localizes to puncta upon HU treatment, but the functional implication of this observation is unclear [14] The fact that RGG-motif proteins have emerged as important regulators of mRNA fate motivated us to hypothesize that RGG-motifs could contribute to genotoxic stress response in yeast and that such a role could be conserved in human. Our results report an exciting new contribution of yeast proteins Sbp1, Scd6 and its human ortholog LSM14s during the genotoxic stress response.

Results

Scd6 and Sbp1 localize to granules in response to HU stress

Using live cell imaging experiments with tagged proteins, we observed that Scd6 localized to foci upon HU treatment (Figure 1A). A time course experiment revealed that within 45 minutes of 0.2 M HU treatment, the number of Scd6-GFP granules per cell increased from 1 to 2.2 (n=3) (Figure 1B). We wanted to know if localization to foci is specific to Scd6 or general to other RGG-motif proteins. Hence, we shortlisted four more RGG-motif containing RBPs (Sbp1, Npl3, Gbp2 and Psp2) to evaluate their localization in HU-treated cells. Sbp1

and Npl3 (like Scd6) are known to be involved in translation repression activity mediated by binding to eIF4G1 among other known functions [15]. Psp2 has been implicated in promoting translation of specific mRNA in autophagy response [16]. Gbp2 is mainly involved in mRNA export and processing. Npl3 and Gbp2 are shuttling proteins, mainly localised in the nucleus and have known connections to cellular stress response [17,18] Out of the four proteins tested, Sbp1-GFP (like Scd6-GFP) localized to foci in response to HU treatment (Figure 1C) with granules per cell increasing from 0.3 to 0.8 upon 60 minutes of exposure to HU (n=3) (Figure 1D) Unlike Scd6-GFP, Sbp1-GFP formed clear, distinguishable granules at 60 minutes, instead of 45 minutes. No significant change in localization was observed for GFP-tagged Npl3, Gbp2, and Psp2, even after 120 minutes of HU treatment (Figure 1E). Localization of both Scd6-GFP and Sbp1-GFP to granules is not due to increased protein levels upon HU exposure, as indicated by western blot analysis (Figure 1F). Of note, due to technical difficulty associated with detecting Scd6-GFP using anti-GFP antibody, levels of endogenously tagged Scd6-myc were quantified upon HU treatment. Based on these observations we conclude that Scd6 and Sbp1 may have a specific role under HU-induced genotoxic stress.

HU-induced Scd6 and Sbp1 puncta colocalize, require RNA and are reversible

Since both Scd6 and Sbp1 localize to foci in response to HU, we hypothesized that they could colocalize. To test this hypothesis, live cell imaging was done with GFP-tagged endogenous Sbp1 and plasmid borne Scd6-mCherry. We observed that 91% of Sbp1-GFP foci colocalized with Scd6-mCherry foci upon 60 minutes of HU exposure (Figures 2A and 2B). To investigate whether mRNAs were present in the Scd6 and Sbp1 granules formed upon HU treatment, we treated cells with cycloheximide (CHX) which inhibits translation elongation and causes the mRNAs to be stuck in the polysome thereby reducing its availability. This prevents formation of new mRNP granules such as SGs and PBs and also causes dissociation of existing mRNA containing granules. When HU-treated cells were subjected to 1 mg/ml of CHX for 5 minutes at 30 ^{o}C, there was a strong decrease in both Scd6-GFP and Sbp1-GFP granules (Figures 2C and 2D). For Scd6, the granule/cell count decreased from 0.95 to 0.15 (Figure 2D, left panel) whereas for Sbp1 no granules were visible upon CHX treatment (Figure 2D, right panel). This suggests that mRNAs are present in Scd6 and Sbp1 granules that form in response to HU treatment.

RNA granules disassemble rapidly upon removal of stress [19]. The reversible nature of RNA granules is important as it allows the return of mRNAs and various RBPs to the cytoplasm.

To examine if the HU-dependent formation of Scd6 and Sbp1 granules is reversible and therefore dynamic, we performed the experiments as described earlier but followed by a recovery period. During the recovery period, the cells were resuspended in HU-free media and the status of granules was observed. After 75 minutes of recovery, Scd6-GFP granules decreased from 1 to 0.3/cell. Similarly, the number of Sbp1-GFP granules decreased from 0.9 to 0.25 in 90 minutes (Figure 2G). Based on these observations, we conclude that the formation of Scd6 and Sbp1 granules in response to HU is reversible. Since CHX experiments indicated that these granules contain mRNAs, the localization of Scd6 and Sbp1 to these foci subsequently regulates the fate of specific mRNAs in response to HU.

Since discernible Sbp1-GFP puncta become visible (45 min) later than Scd6-GFP puncta (60 min; Figure 1A and C) we tested if Scd6 could affect the localization of Spb1. We observed a significant decrease (from 0.8 to 0.5 granules/cell) in the localization of Sbp1-GFP to granules in the absence of Scd6 *(Δscd6* strain) (Figures 3A and 3C left). No difference in the localization of Scd6-GFP was observed in the absence of Spb1 *(Δspb1* strain) (Figures 3B and 3D left). This was not due to a decrease in protein levels as GFP intensity quantitation indicated a net increase in Sbp1-GFP levels (Figure 3C, right). This suggests that Scd6 is important for localization of Sbp1 to puncta upon HU treatment.

RGG-motif is required for localization of Scd6 and Sbp1 to puncta

Both Scd6 and Sbp1 are multidomain proteins containing a C-terminal and a middle RGG domain, respectively. In addition, Scd6 has an N-terminal Lsm domain, and a middle FDF domain (Figure 4A). Of note, this domain organization is conserved across all Scd6 orthologs. The RGG domain of Sbp1 is flanked by two RRM domains, RRM1 and RRM2 (Figure 4A). RGG-motifs constitute low-complexity sequences implicated in the assembly of RNA granules. Also, since previously characterized function of both Scd6 and Sbp1 were mediated through their RGG domain [6,7], we tested the localization of RGG domain deletion mutant of both Scd6 and Sbp1. We observed that localization of Scd6-GFP to granules decreased by almost 50% when RGG domain is deleted (Scd6-GFP ΔRGG) (Figures 4B and 4C). The Lsm domain of Scd6 is reported to bind RNA as well as protein. When the Lsm domain was deleted (Scd6-GFP ΔLsm), the localization of Scd6-GFP to granules was almost completely abrogated indicating that the Lsm domain is essential for Scd6 localization to granules (Figure 4B). Interestingly, deletion of Spb1 RGG domain (Spb1-GFP ΔRGG) caused complete cessation of Sbp1 granule localization and it was similar to the effect

observed with the Lsm domain deletion mutant of Scd6. These observations suggest that although the absence of Lsm domain of Scd6 completely compromises its ability to localize to puncta, the RGG-motif of both Scd6 and Sbp1 is important for their localization to puncta.

Scd6 modulates cellular tolerance to HU

To test the physiological role of Scd6 and Sbp1 in the response to HU, we measured growth kinetics of Δ*scd6* and Δ*sbp1* strain upon HU treatment. We observed that both Δ*scd6* and Δ*sbp1* strains grew marginally but significantly better than the wild type (WT) strain in the presence of HU (Figures 5A and B). Consistent with this observation, we observed an increase in the CFUs of both Δ*sbp1* and Δ*scd6* strains on HU containing media as compared to WT (Figure 5C). Taken together these observations indicate that Scd6 and Sbp1 contribute to HU-stress response pathway(s).

We further observed that absence of Scd6, but not Sbp1, significantly increased the sensitivity of cells to HU upon SRS2 overexpression using a CEN plasmid under its own promoter (Figures 5D and 5E). SRS2 is 3'-5' DNA helicase involved in the regulation of homologous recombination (HR)[20]. SRS2 levels are tightly regulated and overexpression of SRS2 causes growth defect and increases sensitivity to genotoxic stress[21]. Excess SRS2 causes the formation of toxic intermediates upon checkpoint activation and initiation of HR mediated repair [22]. Altogether, Scd6 appears as being an important player in in the genotoxic stress response.

LSM14A localizes to puncta upon both HU and cisplatin treatment in an RGG-motif dependent manner

To analyze if the role Scd6 was conserved in human, we focused on LSM14A, the human ortholog of Scd6, that is also known to localize to P-bodies and to repress translation [23]. Of note, Sbp1 has no known human ortholog. Like Scd6, LSM14A is a modular protein (Figure 6A) with two RGG domains. Using immunofluorescence imaging, we saw that LSM14A localized to puncta upon HU treatment (Figures 6B and 6C). Since the presence of an RGG motif was important for the localization of Scd6 and Sbp1 to granules, we next tested the role of the RGG-motifs in the localization of LSM14A to puncta. Deletion of the two RGG-motifs of LSM14 (LSM14A ΔRGG1 ΔRGG2) led to a decreased localization to puncta (Figures 6D and 6E). The same was observed following treatment with Cisplatin (Figures 6F to 6I),

showing that the requirement for the RGG-motifs-dependent localization of LSM14A to puncta is not specific to HU.

LSM14A modulates translation upon genotoxic stress

To better understand the role of LSM14A in translation control, we used a polysome profiling approach. RNAs isolated from translating (heavy) and non-translating (light) fractions of wild type and LSM14A knockdown (siRNA) cells were sequenced to identify mRNAs whose association with polysomes was perturbed by LSM14A. 112 mRNAs were identified to be differentially regulated (Figure 7A). Of these, association to polysomes of 66 mRNAs was decreased whereas the association of 46 mRNAs was increased. To address the role of LSM14 in the HU response, similar analysis was carried for LSM14A-depleted cells treated with HU (Figure 7B). 163 mRNAs were identified to be differentially regulated at the translation level. Of these, 77 mRNAs were found to be differentially upregulated (Figure 7C), and 86 mRNAs were differentially downregulated (Figure 7D). These observations suggest a role of LSM14A in translation control under normal conditions as well as under genotoxic stress.

Gene ontology (GO) analysis of mRNAs that are differentially upregulated in knockdown of LSM14A upon hydroxyurea revealed DNA damage response category consisting of transcripts such as XRCC4/5/6, NHEJ, ATM and LIG4 (Figure 7C). This suggests LSM14A plays an important role in regulating translation of mRNAs involved in the DNA-damage repair pathway upon genotoxic stress. Amongst others, we also observed categories such as chromosome maintenance and cell development (Figure 7C). We decided to validate a transcript each from DNA damage (LIG4), chromosome maintenance (SASS6) and cell development (FAM111B) categories. The proteins encoded by each of these transcripts have been implicated in genotoxic stress response and genome stability (see Discussion).

We found several categories of mRNAs that are differentially downregulated in the knockdown of LSM14A upon hydroxyurea stress (Figure 7D). Few major categories include cell signaling/signal transduction, regulation of transcription and ubiquitin conjugation pathway. Surprisingly transcripts such as RAD1/9A/9B belonging to the DNA damage response category are also downregulated. The mechanism and consequence of downregulation of above genes in LSM14A mediated genotoxic stress response will be explored in future.

We validated changes in association to polysomes of 3 transcripts using RTqPCR-based quantification of specific mRNAs in polysome fractions. These include the mRNAs encoding LIG4 (DNA Ligase IV), SASS6 (SAS-6 centriolar assembly protein) and FAM111B (FAM111 trypsin-like peptidase B). These mRNAs shifted from light to heavy polysome fractions upon HU treatment and LSM14A knockdown (Figure 8A-C). This result validates the RNA seq observation that HU treatment upregulates the translation of these mRNAs in LSM14A-depleted cells.

Discussion

In this report we have explored and identified a conserved role of RGG motif-containing proteins in the response to HU. Several observations support this conclusion: (i) Sbp1, Scd6 and its human homolog LSM14A localize to puncta upon HU-induced genotoxic stress, (ii) Localization of Sbp1 to HU-induced puncta is partially dependent on Scd6 localization, (iii) The RGG domains of Scd6, Sbp1 and LSM14A are important for their localization to granules, (iv) The absence of both Scd6 and Sbp1 decreases HU sensitivity, (vi) The absence of Scd6 increases sensitivity to HU upon SRS2 overexpression (vii) LSM14A regulates translation of multiple transcripts including those important in the genotoxic stress response to HU. These results identify an exciting new role of RGG motif-containing proteins in the genotoxic stress response.

RNA granules are sites of regulation of mRNA translation and decay. Localization of Sbp1, Scd6 and LSM14A to puncta upon HU treatment suggests that such localization could lead to regulation of mRNA fate upon HU stress. Consistent with this, the elongation inhibitor cycloheximide significantly decreases Scd6 and Sbp1 puncta upon HU stress. The reversibility of HU-induced Scd6 and Sbp1 puncta suggests that resident mRNAs may return to translation once the stress is removed.

Our study emphasizes a conserved role of RGG-motifs in HU stress response. RGG-motifs have been implicated in several cellular processes including translation control. Localization of Sbp1, Scd6 and LSM14A to puncta is dependent on their RGG-motif as the mutants lacking this motif are defective in localizing to puncta [6,7,23] RGG-motifs are unique as these have been implicated in both assembly and disassembly of RNA granules [24–26] It must be noted that the Lsm domain of Scd6 has the strongest impact on localization of Scd6 to HU-induced puncta (Figure 4A). The interactions of RGG-motif with RNA and/or proteins that enable localization of these proteins to puncta remain to be explored.

The demonstration of LSM14A affecting the translation status of mRNAs was missing. Through polysome profiling experiments we have identified several transcripts regulated by LSM14A upon HU stress (Figure. 7). We have validated changes in the translation status of three such mRNAs, *LIG4, SASS6* and *FAM111B* (Figure 8A-C). LIG4 (DNA Ligase IV) associates with XRCC4 to promote DNA double strand break repair via the non-homologous end joining (NHEJ) pathway. Our data suggests that under normal conditions, the translation of the *LIG4* mRNA is repressed by LSM14A. In response to genotoxic stress such as HU, it is derepressed to help the cell to mount a genotoxic stress response (Figure 8A). An interesting future direction would be to study the mechanism that allows repression and de-repression of the translation of the *LIG4* mRNA by LSM14A. We think that the repression mechanism of LSM14A is likely similar to Scd6 which targets eIF4G to repress translation [15] Consistent with this is our observation that LSM14 is in physical proximity with eIF4G using proximity ligation assays (Supplementary Figure 2).

RNA sequencing data reveals that HU treatment of LSM14A knockdown cells leads to downregulation of homologous recombination pathway components (like RAD9, RAD1 and HUS1B)[27], and upregulation of non-homologous end joining and nucleotide excision repair components (like LIG4, ERCC1, ERCC4, XRCC4 etc.)[28] . It seems that LSM14A is involved in directing the DNA damage response to less error-prone homologous recombination mediated repair thus preserving genomic integrity. This observation highlights the possibility that LSM14A could contribute to the decision regarding the kind of DNA damage repair response the cell choses to repair genomic insults such as the one inflicted by hydroxyurea.

SASS6 (SAS-6 Centriolar assembly protein) is a central component of centrioles which plays an important role in its duplication and function. SASS6 is known to promote the growth of esophageal squamous carcinoma cells [29]. Consistent with this observation knockdown of SASS6 decreases proliferation of triple negative breast cancer cells [30]. HU is known to induce centriole amplification which leads to genome instability. We observe that SASS6 is derepressed in absence of LSM14A upon HU stress suggesting that LSM14A functions to keep SASS6 levels under control (Figure 8B).

FAM111B (homolog of FAM111A) belongs to a family of serine protease. This family has been implicated in the clearance of DNA-protein crosslinks (DPC) upon genotoxic stress. DPCs interfere with several cellular processes such as replication, transcription, and recombination [31]. Therefore, the DPC proteases like FAM111B play an important role in maintaining genomic stability. Evidence suggest that deregulated levels of FAM111A/B proteases are detrimental to cells [32]. Our study identifies LSM14A as a translation regulator

which keeps levels of FAM111B under control (Figure 8C) suggesting that LSM14A could play a role in maintaining genomic stability by maintaining DPC clearance.

Interestingly absence of Scd6 and Sbp1 affects the ability of cells to deal with HU stress. Both deletion strains increase the tolerance of cells towards HU. This is evident based on the results obtained from the growth curve and CFU experiments (Figure 5A, 5B and 5C). We interpret these results to indicate that Scd6 and Sbp1 are likely involved in repression of the translation of mRNAs encoding proteins important for mounting a stress response to HU. This is consistent with results obtained using LSM14A which represses translation of mRNA encoding proteins such as Ligase 4 and FAM111B. Both these proteins have been implicated in maintaining genomic stability in response to HU stress.

Another exciting new link between RGG-motif protein and the genotoxic stress response presented in this study is the observation that Scd6 regulates SRS2 activity. In the absence of Scd6 and upon Srs2 overexpression, cells are more sensitive to HU (Figure 5D & E). Under our experimental conditions, Srs2 overexpression or Scd6 deletion alone does not render any sensitivity to HU compared with WT. Srs2 is a tightly regulated protein[21]. It is a key player in homologous recombination and repair [20,33], therefore any alteration in its levels beyond a certain limit are likely to initiate a signalling cascade leading to its feedback inhibition. HU induces Srs2 overexpression[34]. Since strong overexpression (from galactose-inducible promoter) of Srs2 leads to cellular toxicity (Supplementary Figure 1), we believe that Scd6 functions to keep its level under control upon HU stress. Therefore, the absence of Scd6 leads to increased growth defect upon HU treatment. The mechanism underlying regulation of Srs2 function by Scd6 will be an exciting future direction.

Overall, this study establishes RGG motif-containing proteins Sbp1, Scd6 and LSM14A as a regulator of genotoxic stress response. Identifying the regulatory mechanisms that enable genotoxic stress condition-specific repression activity of LSM14A would be a key future direction. It must be noted that both LSM14A and its ortholog Scd6 are known to be methylated at their RGG-motifs [6,35]. Arginine methylation is known to promote the repression activity of RGG-motif proteins [6,7]. Interestingly, the LSM14A-eIF4G physical proximity depends on arginine methylation (Supplementary Figure 2) as reported for the Scd6-eIF4G interaction. Whether arginine methylation of LSM14A modulates its repression activity in response to genotoxic stress will be important to test in the future.

Methods and materials

Yeast transformation

Strains were grown to 0.6 OD_{600} in complete media and pelleted down. The cells were washed once with water followed by 100 mM Lithium Acetate (LiAc). The cells were resuspended in 100 mM Lithium Acetate and aliquoted into 50 µL fractions. The cell suspension was then layered with 240 µL of 50 % PEG (v/v), 36 µL of 1 M LiAc and 25 µL of salmon sperm DNA (100 mg/ml) and vortexed. The mixture was then incubated in 30 ^{o}C for 30 minutes followed by 15 minutes of heat shock at 42 ^{o}C. The cells were then pelleted, resuspended in 100 µL water and plated on synthetic defined media lacking Uracil (SD-Ura^{-}) glucose, agar plate. The plates were incubated at 30 ^{o}C for 2 days, before colonies appeared.

HU treatment

Yeast cultures were grown in 10 ml of SD-Ura^{-}with glucose as the sugar, to 0.3-0.4 OD_{600} and split into two equal parts. The fractions were treated with 0.2 M HU or water (control) and incubated for 45 minutes (for Scd6) or 60 minutes (for Sbp1) at 30 ^{o}C with constant shaking.

Cycloheximide treatment

Yeast cultures were grown in 10 ml of SD-Ura^{-} with glucose as the sugar, to 0.3-0.4 OD_{600} and split into three equal parts of 2.760 ml each. To two fractions, 240µL of 2.5 M HU was added and to one fraction, same volume of water was added (control). They were incubated for 45 or 60 minutes (depending on the strain) at 30 ^{o}C with constant shaking. After incubation, to the HU containing fractions, 3µL of 100 mg/ml Cycloheximide solution (dissolved in methanol) or methanol (control) was added. Cells were kept back in the shaker for 5 minutes followed by pelleting and live cell imaging.

Yeast Live Cell imaging

In all cases for yeast live cell imaging, after the incubation period, the cells were immediately harvested (14000 rpm, 15 seconds), spotted on glass cover slip (No.1) and observed using live cell imaging. Yeast images were acquired using a Deltavision RT microscope system running softWoRx 3.5.1 software (Applied Precision, LLC), using an Olympus 100×, oil immersion 1.4 NA objective. The Green Fluorescent Protein (GFP) channel had 0.2 or 0.25 seconds of exposure (for Scd6GFP and Sbp1GFP respectively) and 32 % transmittance. Minimum 80 -100 cells were observed for each experiment. Quantification was done as granules per cell. Statistical analysis was done using GraphPad Prism Version 7.0. Statistical significance was calculated using two tailed paired t-test.

Western Blotting

SDS Polyacrylamide gels were transferred onto Immobilon-P Transfer Membrane® (MERCK) using Transfer-Blot® Semi Dry apparatus (BIO-RAD). Transfer was done at 10 V for 1 hour.

Antibodies used in this study	**Catalogue No.**
Anti-Sbp1	Generated in lab
Anti-Pgk1	Abcam, ab113687
Anti-myc	Sigma, C3956
Anti-Rabbit	Jackson ImmunoResearch Laboratories, Code No. 111-035-003
Anti-Mouse	Jackson ImmunoResearch Laboratories, Code No. 115-035-003
Monoclonal mouse LSM14A antibody	SantaCruz Biotechnology, sc-398552
Rabbit EIF4G antibody	Cell Signalling Technologies, 2498
Mouse EIF4E antibody	Cell Signalling Technologies, 9742
Secondary mouse AlexaFluor 594 antibody	ThermoFisher , A32744

Growth curve, Plating assay and Spot assay

For growth curve, secondary yeast cultures were grown to mid-log phase (0.4 to 0.6 OD_{600}). The cells were then sub-cultured in fresh media to a final density of 0.1 OD_{600}. The culture was then split into two parts, one treated with 0.2 M HU (final concentration) and the other part with water (vehicle control). 200 µl of culture was aliquoted from each tube into 96 well clear plate (Corning® Costar Clear Polystyrene 96-Well Plates, Cat ID: 3370). The plate was then incubated in plate reader (Tecan Infinite 200 PRO), at 30 ºC, with 40 seconds orbital shaking (4 mm) every one hour. Readings were recorded every one hour for 24 hours. The data was analyzed and plotted using GraphPad Prism 5.

For spot assay, freshly grown yeast cells from agar plate were resuspended in autoclaved deionized water and serially diluted to 10-fold dilutions after normalizing the first dilution to OD_{600} = 1. 10 µl of each dilution was spotted on agar plate and incubated at 30 ºC for 48-60 hours before imaging. For plating assay, 100 µl of the 4^{th} dilution i.e., 10^{-4} OD_{600} was plated on Control or 100 mM HU containing agar plate. The plates were then incubated at 30 ºC for 48-60 hours before counting the colony forming units (cfu).

Cell culture

The REP-1, hTERT-immortalized retinal pigment epithelial cell line and A2058 melanoma cell line used in this study were purchased from the ATCC. Cancer cell lines were maintained at 37 °C and 5% CO_2 in a humidified atmosphere and grown in DMEM:F12 or MEM growth media supplemented with 10% FBS, 2 mM glutamine, 50 u ml^{-1} penicillin and 50 mg ml^{-1} streptomycin (Gibco)

Immunofluorescence assay

For immunofluorescence experiments to investigate the localization of endogenous LSM14A upon genotoxic stress. Cells were seeded on coverslips pre□coated with 1 µg/ml fibronectin (Sigma) and 20 µg/ml collagen (Sigma) two day before treatment with genotoxic stress agent. After reaching confluency cells were then treated with either 10 mM hydroxyurea for 30 minutes or 10 µM of cisplatin for 6 hours. After the treatment the coverslips were washed twice in PBS, let the coverslip dry for 2-3 minutes. The cells were then fixed with 4% PFA in PBS for 10 minutes followed by permeabilization for 10 min at room temperature in PBS containing 0.1% Tween-20 (PBST). The cells were blocked for 20 minutes at room temperature with 5% BSA in PBST (PBST-BSA) followed by probing with primary antibody. The primary anti-LSM14A antibody was diluted 1:100 times in PBST-BSA solution, added onto the coverslip and incubated for 1 hour at room temperature. Cells were then washed twice with PBST. Secondary antibody conjugated with Alexa Fluor™ 594 was diluted to 1:1000 in PBST-BSA solution, added onto the coverslip at room temperature for 1 hour of exposure. Cells were then washed with PBST, followed by one wash with 1X PBS. Cells were let to dry before putting mounting media containing DAPI followed by fixation onto glass slide for confocal microscopy.

For localization experiment with ectopically expressed LSM14A-GFP and LSM14AΔRGG1ΔRGG2-GFP. Cells were seeded on coverslips pre□coated with 1 µg/ml fibronectin (Sigma) and 20 µg/ml collagen (Sigma) two day before treatment with genotoxic stress agent. After reaching confluency cells were then treated with either 10 mM hydroxyurea for 30 minutes or 10 µM of cisplatin for 6 hours. After the treatment the coverslips were washed twice in PBS, let the coverslip dry for 2-3 minutes. The cells were then fixed with 4% PFA in PBS for 10 minutes followed by permeabilization for 10 min at room temperature in PBS containing 0.1% Tween-20 (PBST). Cells were then washed with PBST, followed by one wash with 1X PBS. Cells were dried onto the cover slip before

putting mounting media containing DAPI followed by fixation onto glass slide for confocal microscopy (Leica SPE).

Proximity ligation assay

Interactions between EIF4E and EIF4G (EIF4E–EIF4G) or LSM14A and EIF4G (LSM14A-EIF4G) were detected by in situ proximity ligation assay (PLA) in A2058 melanoma cell lines untreated or treated with hydroxyurea. PLAs were performed on both fixed and permeabilized melanoma cells. The fixed, permeabilized cells were treated identically, and the PLA protocol was followed according to the manufacturers' instructions (Olink Bioscience), with incubation of the primary antibodies at 4 °C overnight. After blocking, the antibodies were used at the following concentrations: for LSM14A (mouse, sc-398552, Santa Cruz Biotechnology, 1:200); for eIF4G (rabbit, 2498; Cell Signaling Technology, 1:200); for EIF4E (mouse, 9742, Cell Signaling Technology, 1:200). PLA minus and PLA plus probes (containing the secondary antibodies conjugated to oligonucleotides) were added and incubated for 1 h at 37 °C. More oligonucleotides were then added and allowed to hybridize to the PLA probes. Ligase was used to join the two hybridized oligonucleotides into a closed circle. The DNA was then amplified (with rolling circle amplification), and detection of the amplicons was carried out using the Brightfield detection kit for chromogenic development or using the Far-Red detection kit for fluorescence. Cell nuclei were stained with 4′,6-diamidino-2-phenylindole (DAPI). The sections were mounted with Olink Mounting Medium. The first results were visualized by confocal microscopy (Leica SPE), and the analysis was supported by Volocity software. To improve the sensitivity of the fluorescence detection, we next used a scanner (Olympus VS120) (magnification 20×; 2-ms exposure for the DAPI channel and 300-ms exposure for the Cy5 channel; 1 pixel = 0.32 μm), and the number of PLA signals per cell was counted (more than three fields) by semi-automated image analysis (ImageJ and OlyVIA).

Polysomal fractionation and microarray experiment.

To understand the translation control effect of LSM14A, we either transfected A2058 cells with scrambled siRNA or siRNA specific to LSM14A cells. We stress the cells with or without 10 mM hydroxyurea for 2 hours, lysed the cells, and carried out polysome profiling. Sucrose density gradient centrifugation was used to separate the sub-polysomal and the polysomal ribosome fractions. Fifteen minutes before collection, cells were incubated at 37

ºC with 100 mg/ml cycloheximide added to the culture medium. Next, cells were washed, scraped into ice-cold PBS supplemented with 100 mg/ml cycloheximide, centrifuged at 3,000 r.p.m. for 5 min and then collected into 400 ml of LSB buffer (20 mM Tris, pH 7.4, 100 mM NaCl, 3 mM MgCl2, 0.5 M sucrose, 2.4% Triton X-100, 1 mM DTT, 100 U ml21 RNasin and 100 mg ml21 cycloheximide). After homogenization, 400 ml LSB buffer supplemented with 0.2% Triton X-100 and 0.25 M sucrose was added. Samples were centrifuged at 12,000g for 10 min at 4 ºC. The resultant supernatant was adjusted to 5 M NaCl and 1 M MgCl2. The lysates were loaded onto a 15–50% sucrose density gradient and centrifuged in an SW41 rotor at 38,000 r.p.m. for 2 h at 4 ºC. Polysomal fractions were monitored and collected using a gradient fractionation system (Isco). We extracted all the RNAs from each polysome fractions. Total RNA was extracted from the four heaviest fractions and the input samples using the TRIzol–chloroform method.

Real-time PCR

RNA from each of the polysome fractions (16 fractions) was isolated using TRIzol LS reagent (TRIzol™ LS Reagent, Invitrogen, Cat ID 10296010) using the manufacturer's protocol. The isolated total RNA was quantified and a total of 1 ug of RNA was used for complementary DNA synthesis. The cDNAs were diluted to 1:10 times from which equal volume (2 ul) cDNA were used along with SYBR green (TB Green Premix Ex Taq II (Tli RNase H Plus); TaKaRa, Cat ID RR820B) and primers (Bioserve, India) for validation of mRNA levels using quantitative real-time PCR (BioRad CFX96 Touch Real-Time PCR Detection System).

RNA interference

Cells were transfected with 20 nM of each siRNA against LSM14A (Dharmacon) and PRMT1 (Dharmacon) using Lipofectamine RNAiMAX Reagent (Life Technologies) following the supplier's instructions.

GO analysis

The gene ontology analysis was performed using the STRING database (https://string-db.org/). STRING is an online tool that provides information about various protein-protein interaction networks and their functional enrichment analysis. After the RNA sequencing analysis, the pool of differentially upregulated or downregulated mRNAs found in siLSM14A

upon HU stress condition was added as an input to the STRING database. The result and analysis from the STRING database are provided in Figures 7C & D).

References

1. Marnett, L. Endogenous DNA damage and mutation. *Trends in Genetics* **17**, 214–221 (2001).
2. Mohanan, G., Das, A. & Rajyaguru, P. I. Genotoxic stress response: What is the role of cytoplasmic mRNA fate? *BioEssays* **43**, 2000311 (2021).
3. Thandapani, P., O'Connor, T. R., Bailey, T. L. & Richard, S. Defining the RGG/RG Motif. *Molecular Cell* **50**, 613–623 (2013).
4. Chowdhury, M. N. & Jin, H. The RGG motif proteins: Interactions, functions, and regulations. *WIREs RNA* (2022) doi:10.1002/wrna.1748.
5. Chong, P. A., Vernon, R. M. & Forman-Kay, J. D. RGG/RG Motif Regions in RNA Binding and Phase Separation. *Journal of Molecular Biology* **430**, 4650–4665 (2018).
6. Poornima, G., Shah, S., Vignesh, V., Parker, R. & Rajyaguru, P. I. Arginine methylation promotes translation repression activity of eIF4G-binding protein, Scd6. *Nucleic Acids Research* **44**, 9358–9368 (2016).
7. Bhatter, N. *et al.* Arginine methylation augments Sbp1 function in translation repression and decapping. *FEBS Journal* **286**, 4693–4708 (2019).
8. Roy, R., Das, G., Kuttanda, I. A., Bhatter, N. & Rajyaguru, P. I. Low complexity RGG-motif sequence is required for Processing body (P-body) disassembly. *Nature Communications* **13**, 2077 (2022).
9. Yang, W. H., Jiang, H. Y., Gulick, T., Bloch, K. D. & Bloch, D. B. RNA-associated protein 55 (RAP55) localizes to mRNA processing bodies and stress granules. *RNA* (2006) doi:10.1261/rna.2302706.
10. Roy, D. & Rajyaguru, P. I. Suppressor of clathrin deficiency (Scd6)—An emerging RGG-motif translation repressor. *Wiley Interdisciplinary Reviews: RNA* **9**, e1479 (2018).
11. Brandmann, T. *et al.* Molecular architecture of LSM14 interactions involved in the assembly of mRNA silencing complexes. *The EMBO Journal* **37**, (2018).
12. Tanaka, K. J. *et al.* RAP55, a Cytoplasmic mRNP Component, Represses Translation in Xenopus Oocytes. *Journal of Biological Chemistry* **281**, 40096–40106 (2006).
13. Li, Y. *et al.* LSm14A is a processing body-associated sensor of viral nucleic acids that initiates cellular antiviral response in the early phase of viral infection. *Proceedings of the National Academy of Sciences* **109**, 11770–11775 (2012).
14. Tkach, J. M. *et al.* Dissecting DNA damage response pathways by analysing protein localization and abundance changes during DNA replication stress. *Nat Cell Biol* **14**, 966–976 (2012).
15. Rajyaguru, P., She, M. & Parker, R. Scd6 Targets eIF4G to Repress Translation: RGG Motif Proteins as a Class of eIF4G-Binding Proteins. *Molecular Cell* **45**, 244–254 (2012).
16. Yin, Z. *et al.* Psp2, a novel regulator of autophagy that promotes autophagy-related protein translation. *Cell Research* (2019) doi:10.1038/s41422-019-0246-4.
17. Santos-Pereira, J. M., Herrero, A. B., Moreno, S. & Aguilera, A. Npl3, a new link between RNA-binding proteins and the maintenance of genome integrity. *Cell Cycle* Preprint at https://doi.org/10.4161/cc.28708 (2014).

18. Poornima, G. *et al.* RGG-motif containing mRNA export factor Gbp2 acts as a translation repressor. *RNA Biology* (2021) doi:10.1080/15476286.2021.1910403.
19. Decker, C. J. & Parker, R. P-bodies and stress granules: possible roles in the control of translation and mRNA degradation. *Cold Spring Harb Perspect Biol* **4**, a012286–a012286.
20. Marini, V. & Krejci, L. Srs2: The "Odd-Job Man" in DNA repair. *DNA Repair* **9**, 268–275 (2010).
21. Bronstein, A., Bramson, S., Shemesh, K., Liefshitz, B. & Kupiec, M. Tight Regulation of Srs2 Helicase Activity Is Crucial for Proper Functioning of DNA Repair Mechanisms. *G3 Genes|Genomes|Genetics* **8**, 1615–1626 (2018).
22. Bronstein, A., Gershon, L., Grinberg, G., Alonso-Perez, E. & Kupiec, M. The main role of Srs2 in DNA repair depends on its helicase activity, rather than on its interactions with PCNA or Rad51. *mBio* (2018) doi:10.1128/mBio.01192-18.
23. Yang, W. H., Jiang, H. Y., Gulick, T., Bloch, K. D. & Bloch, D. B. RNA-associated protein 55 (RAP55) localizes to mRNA processing bodies and stress granules. *RNA* (2006) doi:10.1261/rna.2302706.
24. Schuster, B. S. *et al.* Controllable protein phase separation and modular recruitment to form responsive membraneless organelles. *Nature Communications* (2018) doi:10.1038/s41467-018-05403-1.
25. Godin, K. S. & Varani, G. How arginine-rich domains coordinate mRNA maturation events. *RNA Biology* Preprint at https://doi.org/10.4161/rna.4.2.4869 (2007).
26. Roy, R., Das, G., Kuttanda, I. A., Bhatter, N. & Rajyaguru, P. I. Low complexity RGG-motif sequence is required for Processing body (P-body) disassembly. *Nature Communications* **13**, 2077 (2022).
27. Li, X. & Heyer, W.-D. Homologous recombination in DNA repair and DNA damage tolerance. *Cell Research* **18**, 99–113 (2008).
28. Conlin, M. P. *et al.* DNA Ligase IV Guides End-Processing Choice during Nonhomologous End Joining. *Cell Reports* **20**, 2810–2819 (2017).
29. Xu, Y. *et al.* SASS6 promotes proliferation of esophageal squamous carcinoma cells by inhibiting the p53 signaling pathway. *Carcinogenesis* (2021) doi:10.1093/carcin/bgaa067.
30. Lili, D. U. *et al.* Knockdown of SASS6 reduces growth of MDA-MB-231 triple-negative breast cancer cells through arrest of the cell cycle at the G2/M phase. *Oncology Reports* (2021) doi:10.3892/or.2021.8052.
31. Ruggiano, A. & Ramadan, K. DNA–protein crosslink proteases in genome stability. *Communications Biology* Preprint at https://doi.org/10.1038/s42003-020-01539-3 (2021).
32. Hoffmann, S. *et al.* FAM111 protease activity undermines cellular fitness and is amplified by gain□of□function mutations in human disease. *EMBO Rep* (2020) doi:10.15252/embr.202050662.
33. Niu, H. & Klein, H. L. Multifunctional Roles of Saccharomyces cerevisiae Srs2 protein in Replication, Recombination and Repair. *FEMS Yeast Research* fow111 (2016) doi:10.1093/femsyr/fow111.
34. Liberi, G. Srs2 DNA helicase is involved in checkpoint response and its regulation requires a functional Mec1-dependent pathway and Cdk1 activity. *The EMBO Journal* **19**, 5027–5038 (2000).
35. Matsumoto, K. *et al.* PRMT1 is required for RAP55 to localize to processing bodies. *RNA Biology* **9**, 610–623 (2012).

Acknowledgement

The authors would like to thank Vagner and Rajyaguru labs for their critical inputs and suggestions during this work. The authors would like to thank Won-Ki Huh (Seoul National University) for providing us with *S. cerevisiae* Scd6-myc strain. We would also like to thank Martin Kupiec for kindly gifting pRS316-SRS2 plasmid. We thank Dr. Sunil Laxman for providing us with GAL-SRS2 plasmid. We thank Poornima Gopalakrishna for creating the RGG-deletion mutants of LSM14A.

Funding

This work was supported by the following grants: Department of Science and Technology grant (EMR/2017/001332) from the government of India; India Alliance DBT-Wellcome trust (IA/I/12/2/500625) and DBT-IISc partnership program (BT/PR27952-INF/22/212/2018) to PIR and Institut Curie, CNRS and INSERM to SV.

Competing interests

The authors declare no competing interests.

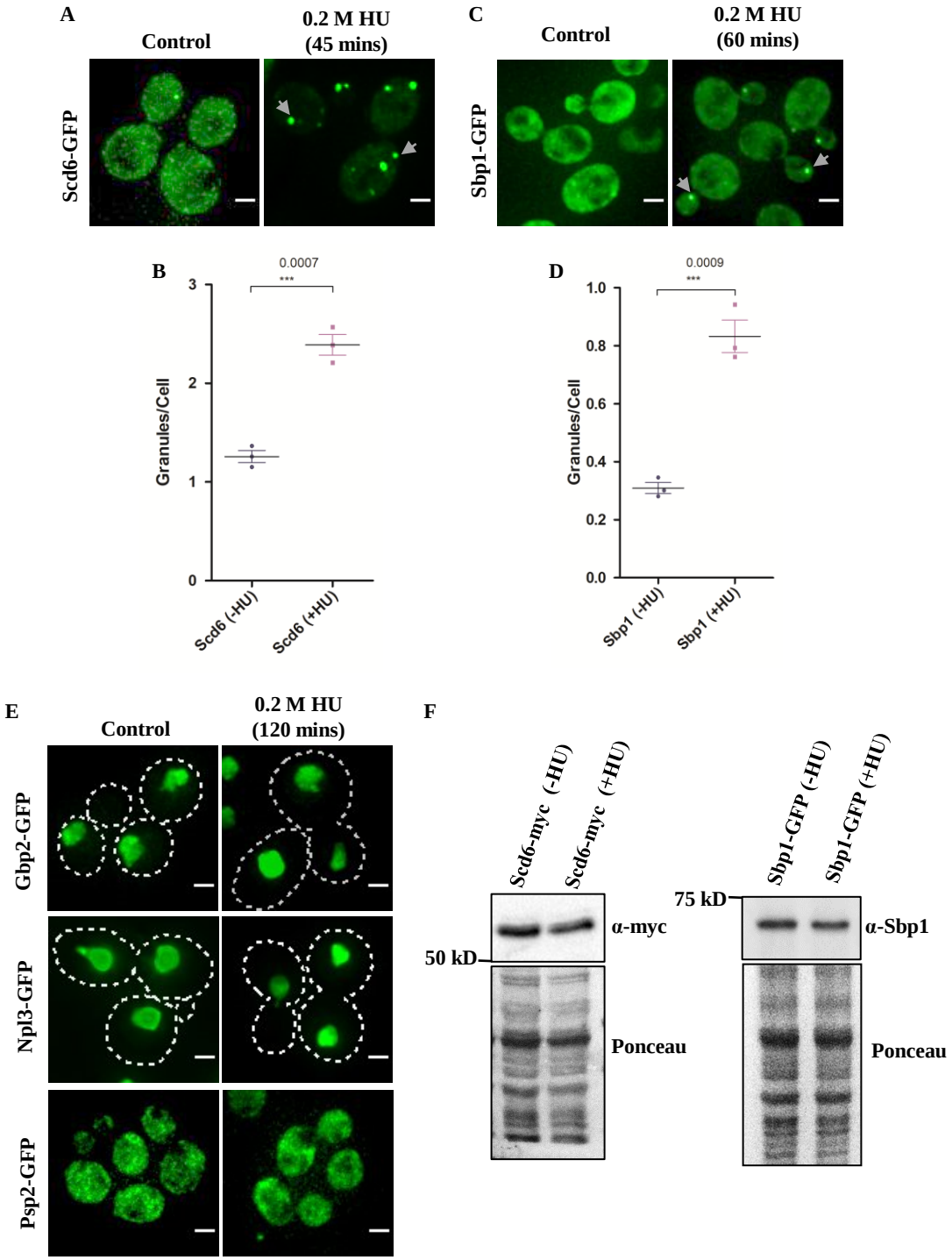

Figure 1. **Scd6 and Sbp1 localize to granules in response to HU.** (A) and (C) Live cell imaging showing localization of Scd6-GFP and Sbp1-GFP to granules upon HU treatment. (B) and (D) Quantification of granules as granules per cell (n=3,~300 cells were counted for each protein). P-values are indicated on the graph and were calculated using unpaired t-test. (E) Gbp2, Npl3, and Psp2, another set of RGG motif-containing RNA binding proteins, do not show change in localization to granule even after 120 mins of HU treatment. (F) Western blot showing protein levels of tagged Scd6 and Sbp1 proteins upon HU treatment. Ponceau stained gel was used as loading control. Scale bar denotes 2 μm.

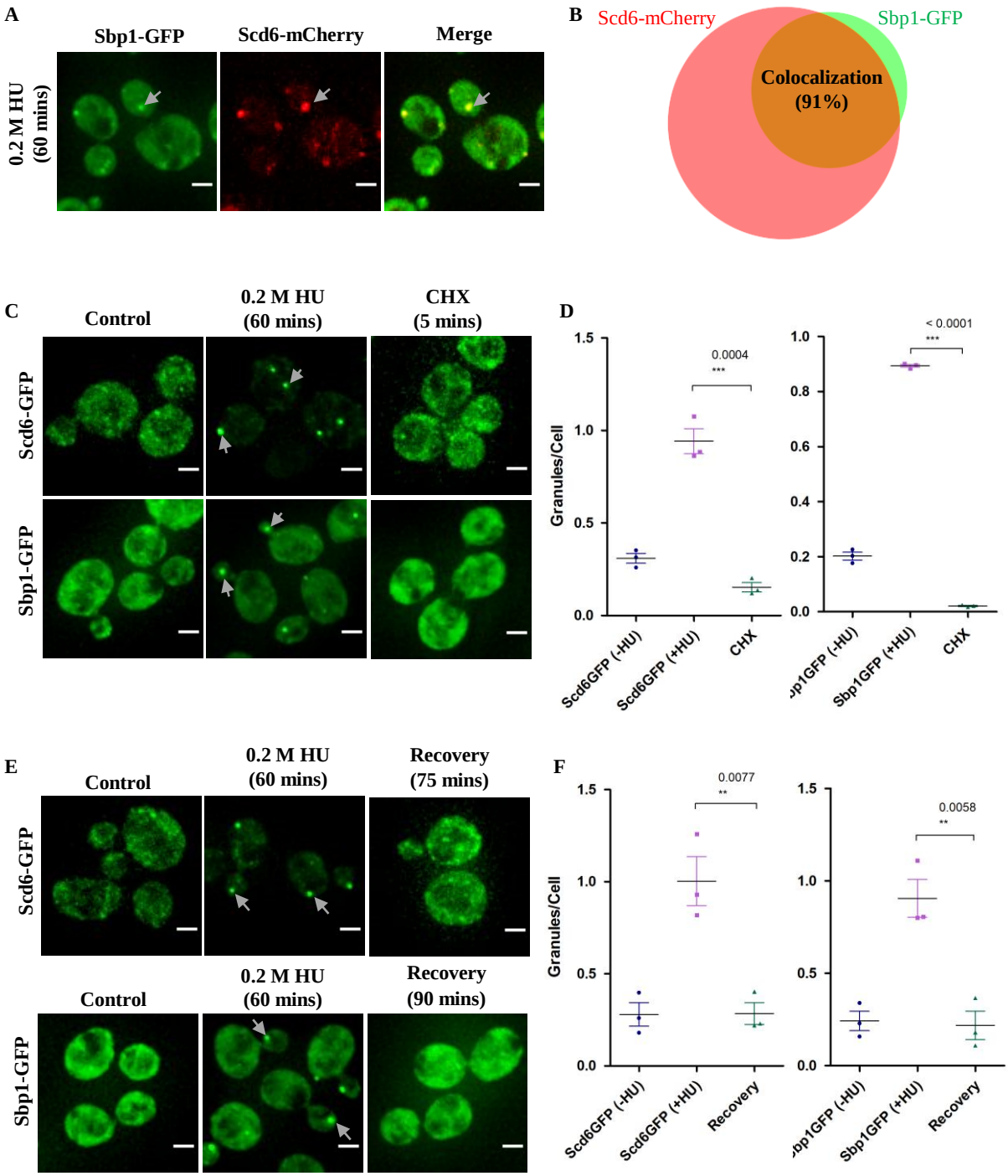

Figure 2. Scd6 and Sbp1 form reversible, RNA containing granules upon HU treatment. (A) Live cell imaging showing colocalization of Sbp1 and Scd6 granules in HU-treated cells. (B) Venn diagram showing colocalization of Scd6-mCherry and Sbp1-GFP granules (Red denotes Scd6-mCherry granules and green indicates Sbp1-GFP granules. Brown colour indicates colocalizing granules. ~90% of Sbp1 granules colocalize with Scd6 granules upon 60 mins of HU treatment (n3; ~300 cells were counted). Percentage colocalization was calculated by dividing total co-localizing foci by total number of Sbp1 foci. (C) Live cell image showing change in localization of Scd6 and Sbp1 after 5 minutes of CHX treatment. (D) Quantification of granules as granules per cell (Left panel shows granule count for Scd6 and right panel for Sbp1). (E) Live cell imaging showing Scd6 and Sbp1 localization after incubating in non-HU containing media (Recovery period is 75 min for Scd6 and 90 minutes for Sbp1). (F) Quantification of granules in terms of granules per cell (Left panel shows change in granules for Scd6 and the right panel shows the same for Sbp1. n=3; ~300 cells were counted for analysis for all experiments. Statistical significance was calculated using unpaired t-test and p- values are indicated on the graphs. Scale bar denotes 2 μm.

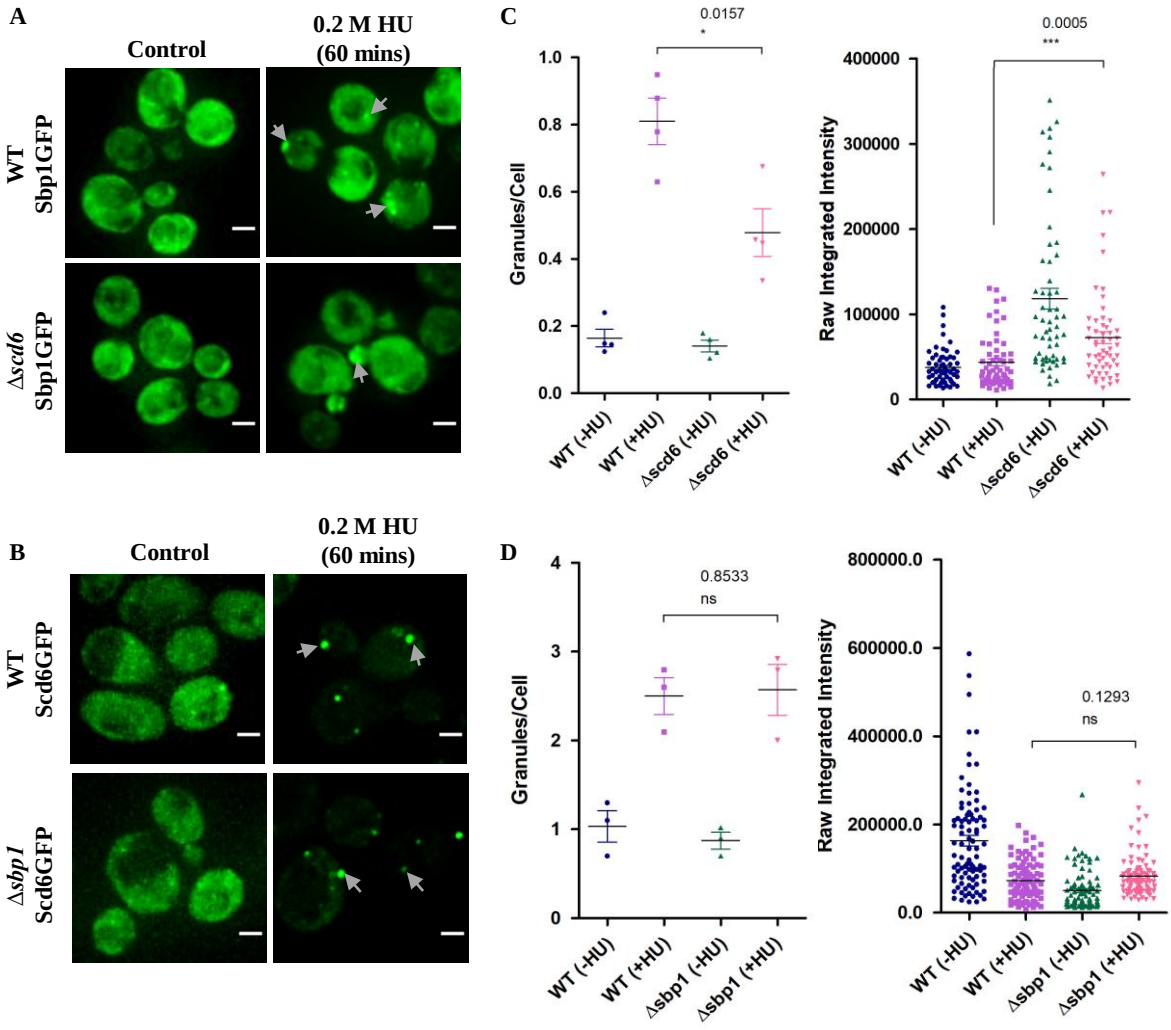

Figure 3. Sbp1 localizes to granules in an Scd6-dependant manner. (A) and (B) Live cell imaging showing localization of Sbp1)GFP and Scd6-GFP in wild type (WT) and *Δscd6* or *Δsbp1* strains, respectively. (C) and (D) Quantification of (A) and (B) as granules/cell and raw integrated GFP intensity (n=3;~400 cells were counted; 100 cells were used for intensity calculations. Statistical significance was calculated using unpaired t-test and p-values are indicated on the graphs (ns: non-significant change). Scale bar denotes 2 μm.

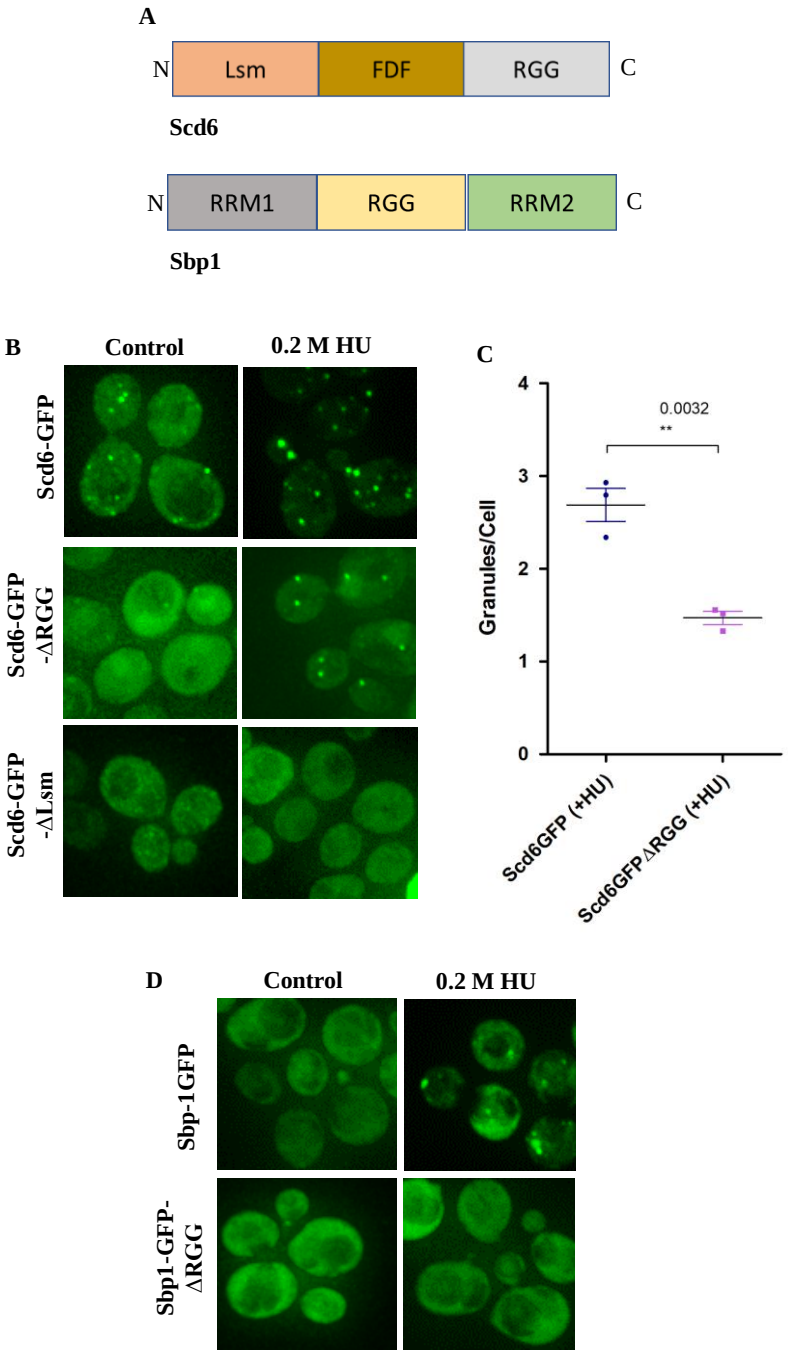

Figure 4. Subcellular localization of Scd6 and Sbp1 domain deletion mutants. (A) Schematic representation shows domain organization of Scd6 and Sbp1. (B) and (D) Live cell imaging showing localization of Scd6 and Sbp1 and their domain deletion mutants upon HU treatment. (C) Quantification of Scd6-GFP WT and ΔRGG mutant granules as granules per cell (n=3; ~300 cells were counted for each protein). Statistical significance was calculated using unpaired t-test and p- values are indicated on the graphs.

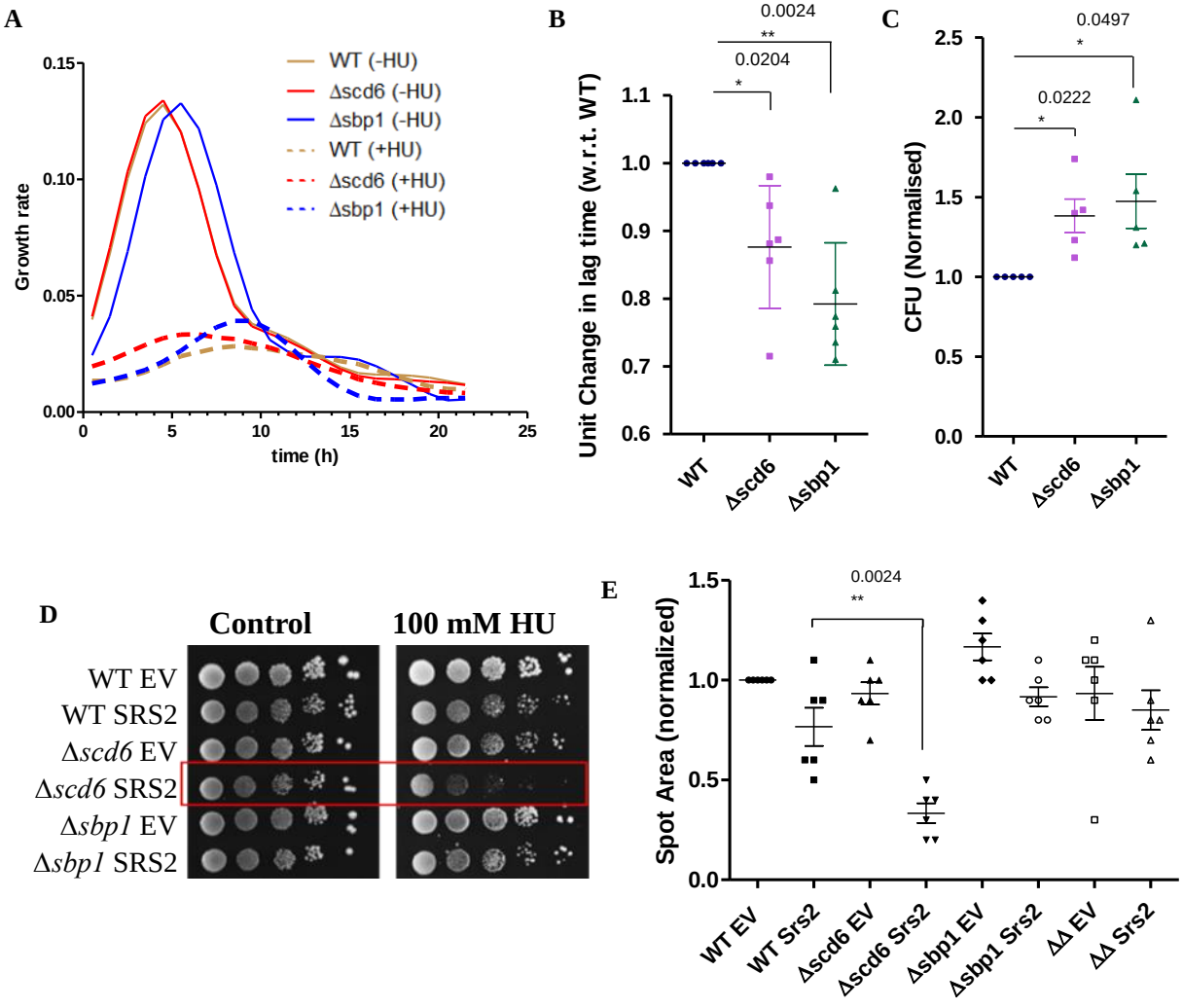

Figure 5. Scd6 modulates cellular tolerance to HU. (A) Representative growth rate curve comparing WT and deletion strains in untreated, and 200 mM HU treated media. (B) Quantification of growth rate in terms of lag time, plotted as change w.r.t. WT (n=6). (C) Quantification of plating assay, plotted as CFUs normalized against WT(n=5). 100 ul of 10^{-4} dilution cell culture were plated on control or 100 mM HU containing YEPD plates. (D) Spot assay of WT and deletion strains either carrying the empty vector (EV) or SRS2 on CEN plasmid, spotted on Uracil dropout agar plate and 2% glucose, in the presence or absence of 100 mM HU. The plates were incubated in 30ºC. (E) Quantification of growth assay by measuring the intensity of the second spot and normalizing the values of spots on HU plate to the respective control values for each strain (n=5).

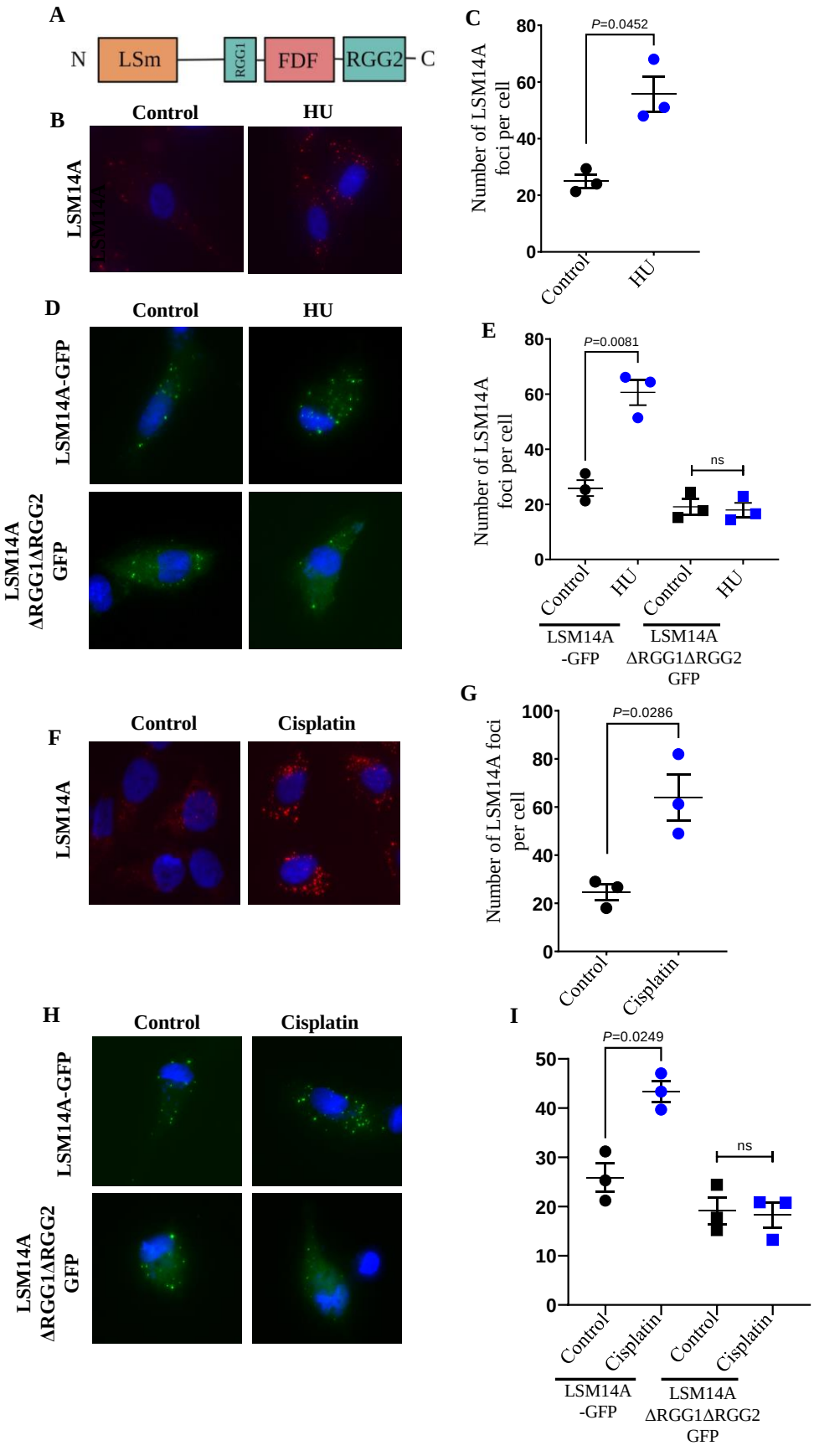

Figure 6: LSM14a localizes to puncta upon genotoxic stress in RGG-motif dependent manner. (A) Domain organization of LSM14A. LSM14A contains a N-terminal LSm domain, a FDF motif and two RGG motifs flanking the FDF motif. (B) Localization of LSM14A in response to hydroxyurea treatment (considered as genotoxic to cells) in the cytoplasm of RPE cells. (C) Quantitation of LSM14A localization as depicted in B. (D) Localization of LSM14A RGG-deletion mutants upon hydroxyurea treatment. (E) Quantitation of localization of LSM14A RGG-deletion mutants as depicted in D. (F) Localization of LSM14A in response to cisplatin treatment in the cytoplasm of RPE cells. (G) Quantitation of LSM14A localization as depicted in B. (H) Localization of LSM14A RGG-deletion mutants upon cisplatin treatment. (I) Quantitation of localization of LSM14A RGG-deletion mutants as depicted in D.

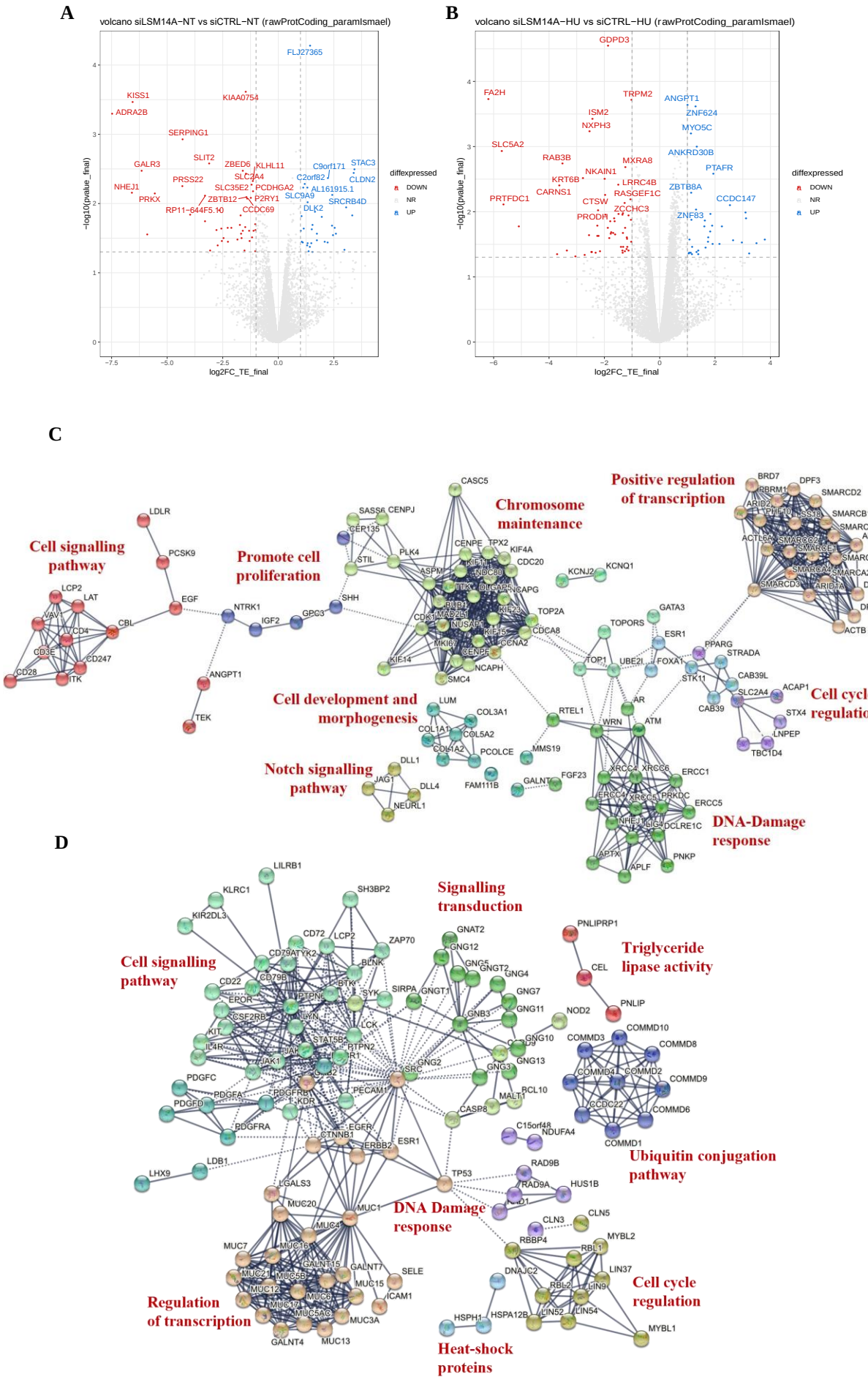

Figure 7: Polysome profiling reveals several mRNA targets of LSM14 under normal (NT) and HU-treated conditions. (A) Volcano plot showing showing changes in transcript levels in siLSM14a knock down cells as compared to wild type cells. (B) Volcano plot showing showing changes in transcript levels in siLSM14a knock down cells as compared to wild type cells upon HU treatment. (C) Gene Ontology analysis of mRNAs that are differentially upregulated in siLSM14A upon genotoxic stress. (D) Gene Ontology analysis of mRNAs that are differentially downregulated in siLSM14A upon genotoxic stress.

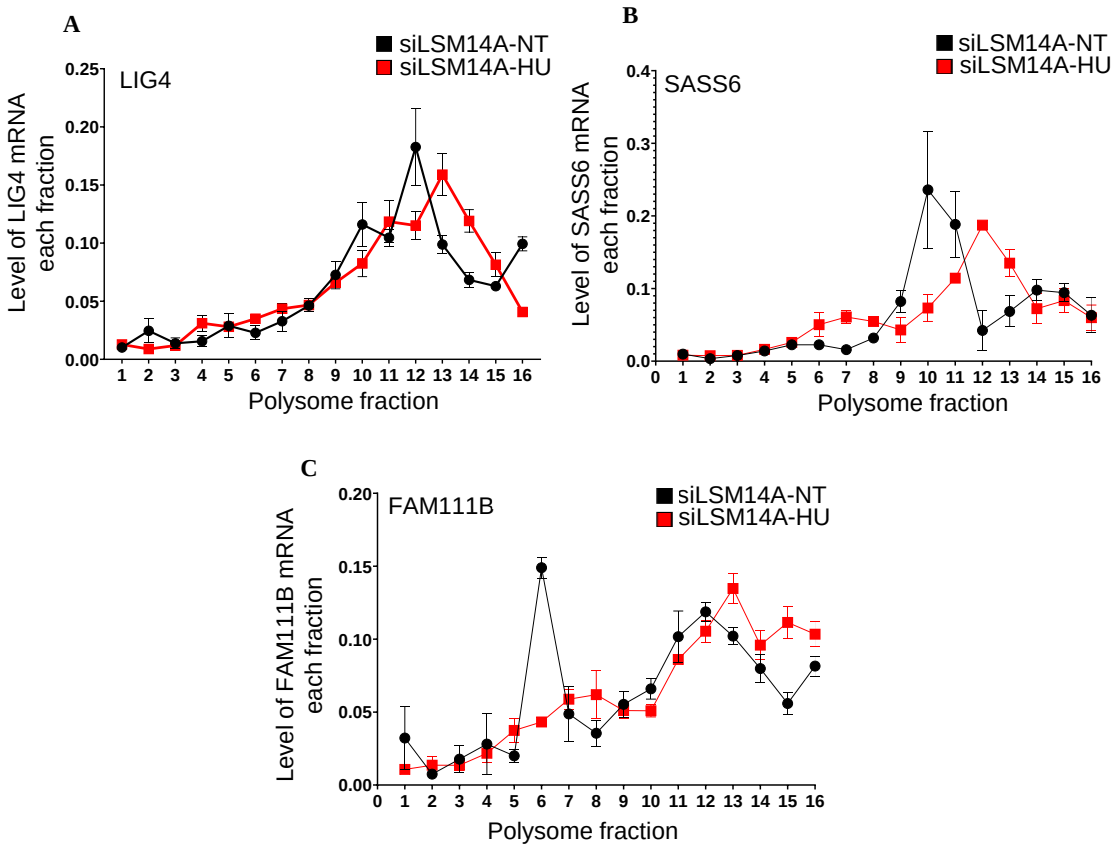

Figure 8: Validation of targets mRNAs identified through polysome RNA sequencing from A2058 cells. (A) Validation of *LIG4* mRNA in each of the polysome fraction comparing siLSM14A untreated (NT) condition with siLSM14A hydroxyurea (HU) treated condition. (B) Validation of *SASS6* mRNA in each of the polysome fraction comparing siLSM14A untreated (NT) condition with siLSM14A hydroxyurea (HU) treated condition. (C) Validation of *FAM111B* mRNA in each of the polysome fraction comparing siLSM14A untreated (NT) condition with siLSM14A hydroxyurea (HU) treated condition.